C. R. Mecanique 341 (2013) 372–377

Contents lists available at SciVerse ScienceDirect

Comptes Rendus Mecanique

www.sciencedirect.com

10th International Meeting on Thermodiffusion

Measurement of the Soret coefficients in organic/water mixtures by thermal lens spectrometry

Humberto Cabrera [a,b,*], Flaminio Cordido [a], Ana Velásquez [a], Pablo Moreno [a], Eloy Sira [c], Santos A. López-Rivera [d]

[a] *Laboratorio de Óptica Aplicada, Instituto Venezolano de Investigaciones Científicas (IVIC), 5101 Mérida, Venezuela*
[b] *The Abdus Salam International Centre for Theoretical Physics, 34151 Trieste, Italy*
[c] *Centro de Física, Instituto Venezolano de Investigaciones Científicas (IVIC), 1020-A Caracas, Venezuela*
[d] *Laboratorio de Física Aplicada, Universidad de Los Andes (ULA), 5101 Mérida, Venezuela*

ARTICLE INFO

Article history:
Available online 7 March 2013

Keywords:
Thermal lens
Thermal diffusion
Soret coefficient

ABSTRACT

In this work we utilize an alternative optical method based on thermal lens spectroscopy for characterizing the thermal diffusion in binary liquid mixtures. In this method, the thermal lens and the Soret signals are separated by a time interval to determine the Soret coefficients. As a demonstrative experiment, the Soret coefficients of isopropanol/water and acetone/water mixtures have been measured using that variant. Our results were compared with the recently published experimental and theoretical calculations and very good agreement was achieved.

1. Introduction

Thermal diffusion or the Ludwig–Soret effect plays an important role in the understanding of the properties of liquid mixtures [1,2]. It characterizes the flux of matter in response to a gradient in temperature, which leads to the formation of a concentration gradient [3]. This stationary concentration gradient is given by:

$$\nabla c = -S_T c_0 (1 - c_0) \nabla T \tag{1}$$

where $S_T = D_T/D$ is the Soret coefficient, D the mass-diffusion coefficient, D_T the thermal diffusion coefficient, T the temperature, c the molar fraction of component 1 (the heaviest component), and c_0 its equilibrium value [4].

The thermal lens method [TL] is a powerful method that can be used to study the Soret effect in transparent liquid mixtures. The TL measures the amount of heat deposited in a medium after absorption of light. Immediately following absorption of photons, the spatial heat distribution resembles the intensity distribution of the beam spot. Later, thermal diffusion spreads heat over distances more than 1 order of magnitude larger than the excitation beam spot radius. Because the refractive index depends on temperature, a spatial distribution of the refractive index of a similar extent is generated in the absorbing medium. In addition to the temperature-dependent refractive index gradient, the Soret effect can produce refractive index changes and influence the total signal [5]. For cw excitation, the generation of a stationary TL can take milliseconds to several seconds, depending on the beam spot radius and the thermal diffusivity of the sample. The TL alters the propagation of beams through the medium by generating a phase shift of the beam wavefronts. Since the first report of the thermal lens effect, the sensitivity of the technique has been improved by changing the experimental configuration. Early experimental arrangements used a single-beam configuration, which employed one laser beam to excite the TL and probe

* Corresponding author at: Laboratorio de Óptica Aplicada, Instituto Venezolano de Investigaciones Científicas (IVIC), 5101 Mérida, Venezuela.
E-mail address: hcabrera@ivic.gob.ve (H. Cabrera).

1631-0721/$ – see front matter
http://dx.doi.org/10.1016/j.crme.2013.01.011

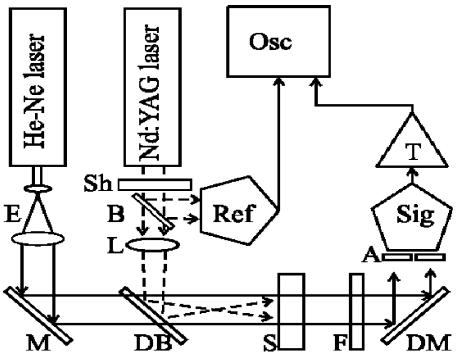

Fig. 1. Experimental setup. E, beam expander; M, mirror; DB, dichroic beam combiner; S, sample; F, interference filter; DM, dichroic mirror; A, pinhole; Sig, photodetector; T, current preamplifier; Osc, digital oscilloscope; Sh, shutter; B, beam splitter; L, lens; and Ref, reference photodetector.

it [6]. The use of a second probe beam for testing the TL has improved the versatility and sensitivity of the technique [7–10]. The dual-beam configuration provides the possibility to use signal processing devices, e.g., lock-in amplifiers, to improve the signal-to-noise ratio and hence the sensitivity of the TL measurement. In addition, detection optics and detectors can be optimized for a single, convenient probe laser wavelength rather than require detection in what may be a more difficult spectral region, which is a convenient choice for generating continuous scanning TL spectra [8].

An advantage of the thermal lens method compared to the diffusion cell is the short duration of a typical experiment (short equilibration times) due to small distances in the order of the focal beam width. Additionally, in thermal lens experiment's typical temperature changes are in the order of 10^{-2}–10^{-5} °C [6,11]. These facts permit to work with extremely small temperature and concentration gradients, so that the addition of dye can be avoided by using the natural absorption of the molecules. Such advantages allow the independence of the Soret coefficient on convection effects. At the same time, sensitivity to convection may be neglected for fast diffusing systems as the water/organic solvents mixtures.

Most of the experiments which utilize the thermal lens effect to measure the Soret coefficient lead only to a qualitative understanding of the Soret coefficients [12], and further improvements in experiments and theory are necessary to obtain reliable values for the thermophoretic properties in all systems, for example isopropanol/water and acetone/water, for which controversial results were published. The aim of this work is to utilize an independent method to determine the Soret coefficients in isopropanol/water and acetone/water mixtures.

2. Description of the experimental technique

The dual-beam thermal lens experimental setup (see Fig. 1) has recently been used for the measurement of the Soret effect [13,14]. The system is composed of two blocks as follows:

1. *Probe beam and recording block*. The He–Ne laser ($\lambda_p = 632.8$ nm, $P_p = 10$ mW, Spectra Physics) generates the probe beam. This beam is transformed by the beam expander E resulting in a 6-mm width collimated probe beam. This beam is reflected by the mirror M, passes through the dichroic beam combiner DB, the sample S (contained in a 1-cm quartz cuvette), and the interference filter F (center wavelength $\lambda = 632.8$ nm, Thorlabs). Afterward, the dichroic mirror DM reflects it towards the 0.3-mm pinhole A and the photodetector Sig (model DET 110/M, Thorlabs). The output signal of the photodetector Sig is transformed by the current preamplifier T (model SR570, Stanford Research Systems) and introduced into the digital oscilloscope Osc (model TDS 3052, Tektronix). At the oscilloscope Osc, the signal is digitized, saved and processed statistically. The radiant flux of the probe beam at the sample surface is 0.2 mW.

2. *Excitation beam block*. The second harmonic of a diode pumped neodymium yttrium aluminum garnet (Nd:YAG) cw laser (model GSF32-200, $\lambda_e = 532.8$ nm, $P_e = 200$ mW, Intelite) delivers the excitation beam through the shutter Sh (model 846, Newport Corporation), the beam splitter B, and the 180-mm focal length lens L to the beam combiner DB, which reflects it to the sample S. The excitation beam passes from the left to the right through the sample cell S. The interference filter F and the dichroic mirror DM block the excitation beam, preventing it from reaching the pinhole A and the photodetector Sig. The beam reflected from the beam splitter B is sensed by the photodetector Ref (model DET 110/M, Thorlabs), which transforms the incident radiant flux into a synchronization signal for the oscilloscope.

In a thermal lens two-beam experiment, the TL signal is usually defined as the relative change in probe transmission through a small aperture located at the far field and on the optical beam axis as [8]:

$$S(z,t) = \frac{I(z,t) - I_0}{I_0} \tag{2}$$

where z is the sample position with respect to the waist of the excitation beam, I_0 the transmittance of the probe beam through an aperture with no excitation beam present, and $I(z,t)$ its transmittance in the presence of the excitation beam.

Considering the Soret effect in liquid mixtures, the time dependent total signal which is the sum of the pure thermal lens plus the Soret concentration lens has been expressed as [13]:

$$S_{\text{total}}(z,t) = S_{\text{th}} - S_{\text{s}} = \frac{P_{\text{e}}\alpha l K(z,t)}{k\lambda_{\text{p}}}\left[\frac{\partial n}{\partial T} - \frac{\partial n}{\partial c} S_T c_0(1-c_0)\Gamma(z,t)\right] \tag{3}$$

with

$$K(z,t) = \arctan\left\{\frac{4m\nu t/t_{\text{c}}}{\nu^2 + [1+2m]^2 + [1+2m+\nu^2]2t/t_{\text{c}}}\right\} \tag{4}$$

$$\Gamma(z,t) = 1 - \sum_{i=1}^{\infty} \frac{4}{(2i-1)\pi} \sin\left[\frac{(2i-1)\pi}{2}\right] \exp\left[-(2i-1)^2 \frac{t}{t_{\text{D}}(z)}\right] \tag{5}$$

where $\nu(z) = (z-a_{\text{p}})/z_{\text{p}} + (z_{\text{p}}/L - z)[1 + (z-a_{\text{p}})^2/z_{\text{p}}^2]$ is the geometrical parameter of the probe beam with a_{p} and z_{p} as the waist position and the Rayleigh parameter, and L is the detector plane position. The quantity m is a dimensionless parameter that accounts for the level of the mode matching between the probe and excitation beams; t and t_{c} are the time and the characteristic thermal time constant. P_{e}, α, l, k, λ_{p} and t_{D} are the excitation power, absorption coefficient, sample cell length, thermal conductivity, wavelength of the probe field and the characteristic mass-diffusion time, respectively.

In a stationary situation, the total signal is related to the Soret coefficient as follows [9,13,14]:

$$S_{\text{total}\infty} = \frac{P_{\text{e}}\alpha l\pi}{k\lambda_{\text{p}}2}\left[\frac{\partial n}{\partial T} - \frac{\partial n}{\partial c} S_T c_0(1-c_0)\right] \tag{6}$$

Eq. (6) provides a relation between the total signal $S_{\text{total}\infty}$ and the Soret coefficient S_T, however the ratio of the Soret signal and the pure thermal lens signal give us a more compact expression [15]:

$$S_T = \frac{\frac{\partial n}{\partial T}}{\frac{\partial n}{\partial c} c_0(1-c_0)} \frac{S_{\text{s}}}{S_{\text{th}}} \tag{7}$$

This simplification leads to a simpler relation in which there are three unknown parameters: the Soret coefficient S_T, the thermal lens signal S_{th}, and the Soret signal S_{s}. By using this equation, the experimental determination of the absorption coefficient is not necessary, which makes it possible to avoid the addition of dye to increase absorption. This particular property also reduces the uncertainty in the determination of the Soret coefficient.

We can obtain the Soret signal S_{s} as the difference between the final steady-state total signal S_{total} and the value of the pure thermal lens signal S_{th} obtained extrapolating the fit of the thermal lens contribution of Eq. (3) in the 0–500 ms range. Finally the Soret coefficient S_T can be calculated according to Eq. (7).

Measurements were taken according to the following procedure: the shutter Sh modulated the beam with a period of 10 s, and for each sample the signal was obtained from the average of 128 recordings at the digital oscilloscope, then we have determined the value of the final steady-state total signal S_{total} according to the definition given in Eq. (2), which permits us to determine S_{th}, S_{s}, and S_T.

In water/isopropanol and water/acetone preparation mixtures, we have used distilled and de-ionized water (with a purity of better than 99 percent), and Fisher Scientific chemical organic components.

3. Results and discussion

The evolution of the total experimental signal with time is shown in Fig. 2 for the water/isopropanol mixture with an initial mass fraction of isopropanol $c_0 = 0.5$ (at 298 K). The thin red line represents the best fit to the experimental data using Eq. (3) and parameters: $\lambda_{\text{e}} = 532.8$ nm, $\lambda_{\text{p}} = 632.8$ nm, $z_{\text{p}} = 100\,000$ cm, $z_{\text{e}} = 0.0001$ cm, $a_{\text{e}} = 0$, $a_{\text{p}} = 0$, $L = 50$ cm, $m = 10\,000$, $\partial n/\partial T = -3.474 \times 10^{-4}$ K^{-1} [16], $P_{\text{e}} = 73$ mW, $\alpha = 2 \times 10^{-4}$ cm^{-1}, $l = 1$ cm, $k = 3 \times 10^{-3}$ W cm^{-1} K^{-1}, $\partial n/\partial c = -0.0364$ [16], $c_0 = 0.5$, with $S_T = -5.2 \times 10^{-3}$ K^{-1}, and $t_{\text{D}} = 1$ s as fitting parameters.

In Fig. 3 we have represented the experimental signal, but the fit was limited to the pure thermal lens signal (first term of Eq. (3)) with the same parameters used in Fig. 2, and with $t_{\text{c}} = 500$ ms. As shown in Fig. 2, the signal first shows a rapid reduction due to the pure thermal lens effect, followed by a further, much slower, decrease due to the buildup of the Soret concentration gradient. Both processes can be easily separated (Fig. 3) because the Soret component builds up with a time constant which is much greater ($t_{\text{d}} = 1$ s) than the characteristic time constant of the thermal lens ($t_{\text{c}} = 500$ ms) [12,13,17,18]. The separation of the time scales allows analysis of the temporal buildup of the pure thermal lens, which is shown in the expanded scale of the inset in Fig. 3. The fit was limited to the short period, typically 500 ms within which mass diffusion is inoperative and the signal is only governed by the temperature-dependent refractive index gradient. The fit allowed the determination of the transient steady-state thermal lens signal ($S_{\text{th}} = -0.036$), from which the Soret signal ($S_{\text{s}} = 0.005$) was taken as the difference between the final steady-state total signal ($S_{\text{total}\infty} = -0.041$) and the steady-state pure thermal lens signal extrapolated from the fit using only the first term of Eq. (3). Then we have determined the Soret coefficient ($S_T = -5.34 \times 10^{-3}$ K^{-1}) by means of Eq. (7) with $c_0 = 0.5$, $\partial n/\partial T = -3.474 \times 10^{-4}$ K^{-1} [16], $\partial n/\partial c = -0.0364$ [16]. The Soret coefficient obtained from the fitting procedure ($S_T = -5.2 \times 10^{-3}$ K^{-1}) does coincide with this calculated by means of Eq. (7) ($S_T = -5.34 \times 10^{-3}$ K^{-1}). This result demonstrates that predictions of the model are in good agreement with experimental data.

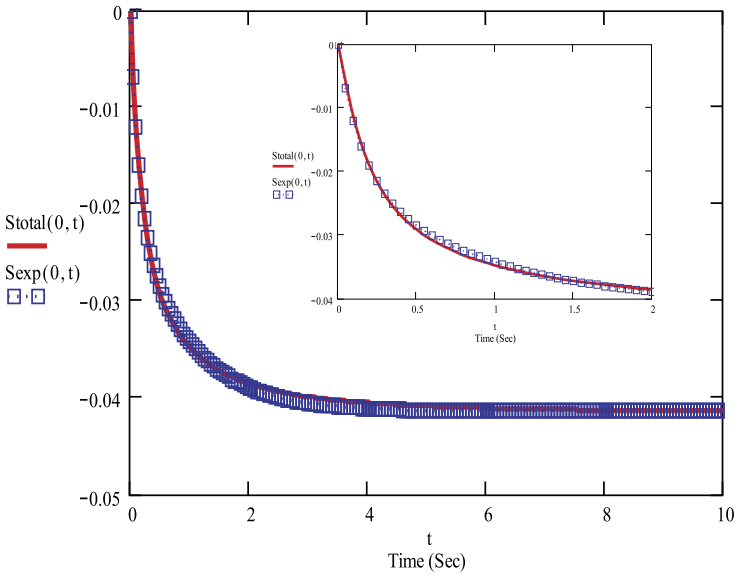

Fig. 2. Time evolution of the total experimental signal ($S_{\text{total}\infty} = -0.041$) for $c_0 = 0.5$, at $T = 298$ K (water/isopropanol system in a 1-cm quartz cuvette). The thin red (in the online version) line is the best fit for the experimental data using Eq. (3). The inset shows the buildup of the total signal in a 2-s initial period with $t_d = 1$ s.

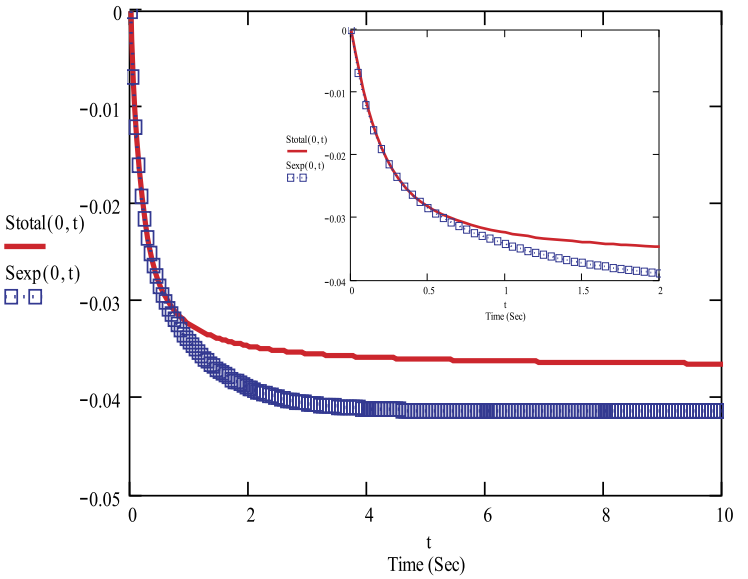

Fig. 3. Time evolution of the total experimental signal for water/isopropanol mixture with $c_0 = 0.5$, at $T = 298$ K. The red (in the online version) line is the best fit for the first term of Eq. (3) with respect to the experimental data and represents the pure thermal lens signal. The inset shows the buildup of the initial thermal lens effect in a 2-s period with $t_c = 500$ ms.

We have applied similar procedure for determining the Soret coefficients for different concentrations of water/isopropanol mixtures and the results are summarized in Fig. 4. In addition to measured and plotted data, Fig. 4 contains also literature data for the Soret coefficients as measured recently by Mialdun et al. [16,19] by three different instrumental techniques, and by Poty et al. [20] many years ago by a flow-cell method. Both results show a reasonable to good agreement with our results in the region $0.2 < c_0 < 0.8$, but there is one exception: the Soret coefficient reported by Poty et al. for $c_0 = 0.7$ deviates significantly from all other data and seems to be too high. In the region with low water content ($c_0 < 0.2$), our results disagree with the previously reported values by Poty. At low water concentration, the contrast factors are very low, which means that concentration variations become invisible for optical techniques and measurements of the transport properties is a difficult task, which is subject to large errors. The results of measurements in this region are not plotted, as they are considered non-reliable. In Fig. 3 we also present a comparison between our experimental values of the Soret coefficient and the prediction of the viscous energy model developed by Abbasi et al. [21]. A rather good agreement is observed.

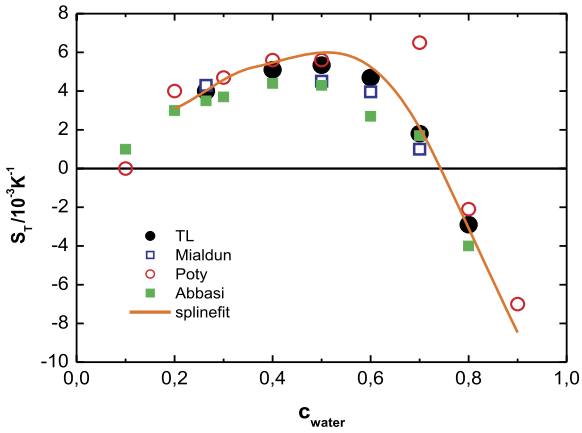

Fig. 4. Soret coefficient of water/isopropanol mixtures as a function of the mass fraction of water in the present work (black circle). The open blue (in the online version) cubes represent the values reported by Mialdun et al. [19] and by Poty et al. [20] by open (red) circles. The full (green) cubes show the prediction of the viscous energy model developed by Abbasi et al. [21]. The (orange) line represents benchmark values that have been obtained from fits of approximating spline functions to all available data [16].

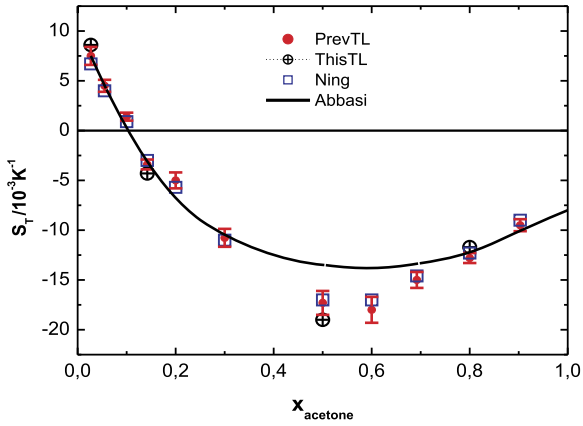

Fig. 5. Soret coefficient of acetone as a function of the molar fraction of organic solvent. The crossed black circles refer to the experimental data measured in this work, and the corresponding solid red (in the online version) circles represent previously reported results [14]. The open (blue) squares are the results reported by Ning et al. [22], and the black line is the prediction of the viscous energy model developed by Abbasi et al. [21].

In Fig. 5, the Soret coefficient S_T is shown as a function of the molar fraction of acetone. It decreases with increasing acetone concentration and reaches a minimum at a molar fraction $x_{\text{acetone}} = 0.5$. For higher acetone concentrations ($x_{\text{acetone}} > 0.5$), S_T increases with x_{acetone}, but for concentrations around $x_{\text{acetone}} = 0.5$, the uncertainties became larger, due to the low value of the contrast factors. For this reason, our own values disagree with the theoretical model developed by Abbasi et al. [21]. In the same figure we have plotted the experimental data reported by Ning et al. [22], and the thermal lens measurements reported previously by our group using another variant of the method [14]. Both results are consistent with the data obtained in the present work. The theoretical model of Abbasi et al. [21] agrees with our experimental data for high and low water contents, but at the minimum of the Soret coefficient, around $x_{\text{acetone}} = 0.5$, measurements lead to the scattering of the results due to the small absolute value of the contrast factor. Both systems (water/isopropanol and water/acetone) show a sign change of the Soret coefficient with concentration. Similar to the case of other aqueous solutions such as methanol/water and ethanol/water, the sign change occurs in the water-rich regions.

4. Conclusions

Soret coefficients of water/isopropanol and water/acetone mixtures have been measured by an optimized thermal lens technique over the wide concentration range. The method does not requires the addition of a small amount of dye, which is an important advantage. For both studied systems, the fitting curves show very good agreement between the theoretical model and experimental data. For water/isopropanol mixtures, our own measurements are consistent with available literature values for the intermediate and high water contents. In the region with low water contents, scattering of the results was obtained due to the small absolute values of the contrast factors. This behavior was reproduced for measurements in the water/acetone system, in which the values of the Soret coefficients also are scattered around $x_{\text{acetone}} = 0.5$ as compared

with the available theoretical model developed by Abbasi. The Soret effect of both systems shows a strong dependence on the composition. Finally, we have shown the usefulness of the thermal lens technique as an additional independent method providing new reliable benchmark data. The thermal lens technique, as other optical methods, becomes very noisy and inaccurate in regions where the concentration contrast factor vanishes.

References

[1] C. Soret, Arch. Sci. Phys. Nat. 2 (1879) 48.
[2] L. Sitzber, Akad. Wiss. Wien Math.-Naturwiss. Kl. 20 (1856) 539.
[3] S.B. Bierlein, A phenomenological theory of the Soret diffusion, J. Chem. Phys. 23 (1955) 10–15.
[4] H. Tyrell, Diffusion and Heat Flow in Liquids, Butterworths, London, 1961.
[5] M. Giglio, A. Vendramini, Appl. Phys. Lett. 25 (1974) 555.
[6] J. Whinnery, Acc. Chem. Res. 7 (1974) 225.
[7] M. Long, R. Swofford, A. Albrecht, Science 191 (1976) 183.
[8] J. Shen, R. Lowe, R. Snook, Chem. Phys. 165 (1992) 385.
[9] A. Marcano, H. Cabrera, M. Guerra, R.A. Cruz, C. Jacinto, T. Catunda, J. Opt. Soc. Am. B 23 (2006) 1408.
[10] H. Cabrera, A. Marcano, Y. Castellanos, Cond. Matt. Phys. 9 (2006) 385.
[11] J. Gordon, R. Leite, R. Moore, S. Porto, J. Whinnery, J. Appl. Phys. 36 (1965) 3.
[12] N. Arnaud, J. Georges, Spectrochim. Acta A 57 (2001) 1295.
[13] H. Cabrera, E. Sira, K. Rahn, M. García-Sucre, Appl. Phys. Lett. 94 (2009) 051103.
[14] H. Cabrera, L. Marti-López, E. Sira, K. Rahn, M. García-Sucre, J. Chem. Phys. 131 (2009) 031106.
[15] P. Polyakov, S. Wiegand, Phys. Chem. Chem. Phys. 11 (2009) 864.
[16] A. Mialdun, V. Yasnou, V.M. Shetsova, A. Königer, W. Köhler, D. Alonso de Mezquia, M.M. Bou-Ali, J. Chem. Phys. 136 (2012) 244512.
[17] N. Arnaud, J. Georges, Spectrochim. Acta A 60 (2004) 1817.
[18] N. Arnaud, J. Georges, Spectrochim. Acta A 69 (2008) 1063.
[19] A. Mialdun, V.M. Shetsova, Int. J. Heat Mass Transf. 51 (2008) 3164.
[20] P. Poty, J.C. Legros, G. Thomaes, Z. Naturforsch. 29A (1974) 1915.
[21] A. Abbasi, M.Z. Saghir, M. Kawaji, J. Chem. Phys. 130 (2009) 064506.
[22] H. Ning, S. Wiegand, J. Chem. Phys. 125 (2006) 221102.